

## Article

# In Silico Evaluation of the PCR Performance of Different Tests for Detection of WSSV

Arturo Sánchez-Paz, Trinidad Encinas-García and Fernando Mendoza-Cano \*

Laboratorio de Virología, Centro de Investigaciones Biológicas del Noroeste (CIBNOR), S.C. (Unidad Hermosillo), Calle Hermosa 101, Fraccionamiento Los Ángeles, Hermosillo 83206, Sonora, Mexico; asanchez04@cibnor.mx (A.S.-P.); tencinas@cibnor.mx (T.E.-G.)

\* Correspondence: fmendoza@cibnor.mx

**Abstract:** In this study, the primers of different protocols for the detection of White Spot Syndrome Virus (WSSV) were analyzed in silico to evaluate their potential performance in PCR. As with any biological entity, this virus evolves constantly. Thus, this analysis showed that a few primers, including those recommended by the World Organization for Animal Health (WOAH), might mismatch with some isolates of WSSV, specially with isolates more recently sequenced. Furthermore, a set of primers recommended by WOAH, showed the potential to self-dimer and form hairpin loop structures, which could affect the efficiency of PCR, resulting in an inaccurate diagnostic result. From our perspective, and considering the evolutionary trajectory of this virus, it may be time for the WOAH to update the PCR protocols recommended for WSSV detection, which remains as a highly prevalent and lethal virus.

**Keywords:** WSSV; WOAH; in silico analysis; primers; viral evolution

**Key Contribution:** To date, several PCR detection methods have been developed to detect WSSV, of which the WOAH only recommends two. Considering that viruses are arguably the fastest-evolving biological entities inhabiting our planet, it is no surprise that some changes on the WSSV genome could adversely affect the performance of some detection tests. Our study shows that some WSSV variants with specific mutations affect the performance of some methods. Thus, the WOAH should incorporate, in the Manual of Diagnostic Tests for Aquatic Animals, new protocols that have confirmed their suitability on the detection of this pathogen in different crustacean species.



**Citation:** Sánchez-Paz, A.; Encinas-García, T.; Mendoza-Cano, F. In Silico Evaluation of the PCR Performance of Different Tests for Detection of WSSV. *Fishes* **2024**, *9*, 5. <https://doi.org/10.3390/fishes9010005>

Academic Editors: Jee Eun Han and Patharapol Piamsomboon

Received: 27 October 2023  
Revised: 15 December 2023  
Accepted: 18 December 2023  
Published: 20 December 2023



**Copyright:** © 2023 by the authors. Licensee MDPI, Basel, Switzerland. This article is an open access article distributed under the terms and conditions of the Creative Commons Attribution (CC BY) license (<https://creativecommons.org/licenses/by/4.0/>).

## 1. Introduction

White spot disease (WSD), provoked by the infection of crustaceans with White Spot Syndrome Virus (WSSV), has been listed as a compulsory notification of aquatic animal diseases by the World Organization for Animal Health (WOAH, formerly known as OIE) since 1997 [1]. Despite more than 30 years since its emergence in China and Taiwan, WSD remains a significant concern for the global shrimp industry [2]. It has been estimated that 40% of tropical shrimp production is lost annually due to infectious diseases [3], and it has been estimated that approximately 60% of these losses have been associated with viral diseases [4]. Thus, recent approximations suggest that WSSV has caused a cumulative loss of some USD 21 billion globally since its emergence [5].

The WSSV, a member of the monotypic family *Nimaviridae* (genus *Whispovirus*), contains a large circular double-stranded DNA genome of ~300 kb. Depending on the isolate, 684 to 507 putative open reading frames (ORFs) on both DNA strands have been identified in the WSSV genome. It has been assumed that only 181–184 of these putative ORFs could encode functional proteins [6,7]. Furthermore, only a few ORFs have shown homology to any known proteins identified in other viruses or cellular organisms [8,9].

A remarkable feature of WSSV is its wide range of potential hosts. To date, nearly 100 species of arthropods have been reported as hosts or carriers of WSSV. In addition, active

forms of WSSV have been detected in non-crustacean species such as rotifers, chaetognaths, mollusks, annelids, and insects [10,11]. With appropriate diagnostic tools for detecting the virus, understanding the infection routes and pathogenesis of WSSV is essential for undertaking control measures against WSSV.

Currently, several tests are available for WSSV detection, including ELISA [12–16], immunochromatography [17], PCR assays [18–25], loop-mediated isothermal amplification [26–30], dark-field microscopy [31], colorimetric assays [32] and others. Among such methods, the WOAHA Manual of Diagnostic Tests for Aquatic Animals recommends only two PCR protocols [18,22] suitable for WSSV detection [33]. It has been reported, however, that in some cases, the protocol proposed by Lo et al. [22] could yield false-positive results [34]. Since WSSV is a notifiable pathogen, false-positive results in WSSV-free zones can trigger potential negative consequences due to economic sanctions from trade restrictions.

PCR-based protocols are arguably the most widely used molecular methods for diagnosing and surveilling pathogens because of their high sensitivity, specificity, and high-throughput capabilities [35]. However, a suitable PCR protocol depends on numerous factors in the amplification reaction that may affect its efficiency. It is well recognized that the success of a PCR reaction is strongly dependent on the appropriate design of the primers [36,37]. Thus, the detection of pathogens demands well-designed primers annealing exclusively to the target DNA sequence; otherwise, poorly designed primers may lead to false-positive or false-negative diagnostic results. Therefore, this study aims to evaluate *in silico* whether the WOAHA-recommended PCR primers for WSSV detection, alongside some primers published in other studies, are effectively designed.

## 2. Materials and Methods

### 2.1. Analysis *In Silico* of Primers for WSSV Detection

The primers used for WSSV detection evaluated in this study are listed in Table 1. According to the authors, these primers were developed to detect or quantify the WSSV load. The primers described by Durand and Lightner [18] and Lo et al. [22], recommended by the WOAHA were also included in the list. The genomic location of each set of primers was mapped against a reference genome reported from the WSSV isolated from southern Taiwan in 1994 by Wang et al. [38] (GenBank accession no. AF440570), using the free-access plasmid editor ApE [39].

**Table 1.** List of oligonucleotide primers used in this study.

Primer	Sequence (5′–3′)	Reference	PCR	Size (bp)
146F1 146R1	ACTACTAACTTCAGCCTATCTAG TAATGCGGGTGTAATGTTCTTACGA	[22]	Nested *	1447
146F2 146R2	GTAAGTGGCCCTTCCATCTCCA TACGGCAGCTGCTGCACCTTGT			
146F2 146R2	GTAAGTGGCCCTTCCATCTCCA TACGGCAGCTGCTGCACCTTGT	[40]	One-step	941
WSS1011F WSS1079R Probe	TGGTCCCGTCCTCATCTCAG GCTGCCTTGCCGGAAATTA AGCCATGAAGAATGCCGTCTATCACACA	[18]	qPCR *	69
RT-WSSV-F154 RT-WSSV-R154 RT-WSSV-TP154 Probe	CCAGTTCAGAATCGGACGTT AAAGACGCCTACCCGTGTTGA TCCATAGTTCCTGGTTTGTAATGTGCCG	[41]	qPCR	154
WSSV341F WSSV341R	TGGCTACATCTGCATTGCTC TAGAGACGTGGCTGGAGAGG	[42]	One-step	341

Table 1. Cont.

Primer	Sequence (5'–3')	Reference	PCR	Size (bp)
P1	ATCATGGCTGCTTCACAGAC	[43]	Nested	982
P2	GGCTGGAGAGGACAAGACAT			
P3	TCTTCATCAGATGCTACTGC			
P4	TAACGCTATCCAGTATCACG			
FQ-P3 (up) FQ-P4 (down)	AAGCATCGTGGAGACTCTTGC GAAGATTCGCCGCTCATACC	[44]	qPCR	129
WSSV-RT1 WSSV-RT2 Probe	TTGGTTTCATGCCCCGAGATT CCTGGTCAGCCCCTTGA TGCTGCCGTCTCCAA	[45]	qPCR	154 (57)
Forward Reverse Probe TP109	CCCACACAGACAATATCGAGAC TCGCTGTCAAAGGACACATC TTCTGTGACTGCTGAGGTTGGAT	[46]	qPCR	109
VP28-140Fw VP28-140Rv	AGGTGTGGAACAACACATCAAG TGCCAACTTCATCCTCATCA	[23]	qPCR	141

\* Primers recommended by the WOA (WOAH 2023).

## 2.2. In Silico Analysis

### 2.2.1. Primer Specificity

The specificity of the primers was assayed using the complete WSSV genome sequences available on GenBank through the Primer-BLAST tool (<https://www.ncbi.nlm.nih.gov/tools/primer-blast/index.cgi> (accessed on 31 May 2023) [47]. The non-redundant (nr) database of GenBank and white spot syndrome virus (taxid: 342409) parameters were selected. The primer specificity stringency restricted each primer to have at least two total mismatches to unintended targets, including at least two mismatches within the last 5 bps at the 3' end. Furthermore, targets having 9 or more mismatches to the primer were ignored. Primer-Blast was last accessed on 9 June 2023.

### 2.2.2. Predicted Melt Curves

The melt profiles of the amplicons generated in silico by each pair of primers using the sequences from Taiwan, Thailand, and China (GenBank acc. Nos. AF440570, AF369029, and AF332093, respectively) were predicted using the uMelt web application (<https://www.dna-utah.org/umelt/quartz/um.php> (accessed on 4 July 2023)) [48]. The uMelt parameters selected for in silico prediction were set as follows: The denaturing temperature range was from 65 °C to 95 °C with high resolution (0.25 °C), and the thermodynamic option was set as Unified-SantaLucia 1998 [49]. Since the concentrations of MgCl<sub>2</sub> are only described in Kimura et al. [43], Leal et al. [21], and Tang and Lightner [42], the melt profiles were simulated using the concentration of monovalent cations [Mono<sup>+</sup>]: 20 mM, the concentration of magnesium (final concentration after dNTPs are subtracted from [Mg<sup>2+</sup>]) at the concentration specified in each method, and 0% of dimethylsulfoxide (DMSO).

### 2.2.3. Phylogenetic Analysis of the Amplicons

In total, 15 WSSV DNA sequences from different geographical regions (Table 2) were retrieved from the NCBI GenBank nucleotide sequence database (<http://www.ncbi.nlm.nih.gov/nucleotide/> (accessed on 6 July 2023)). Subsequently, the encoding sequences amplified by the analyzed primers were aligned using the MAFFT online tool (v7.511) (<https://mafft.cbrc.jp/alignment/server/> (accessed on 6 September 2023)) with the L-INS-i iterative refinement approach and with default settings [50] to identify highly conserved regions within the sequences (Supplemental Material). The alignment robustness was then assessed by implementing the GUIDANCE2 software v2.0.2 (<http://guidance.tau.ac.il/ver2/> (accessed on 13 September 2023)) to compute confidence scores [51]. Subsequently,

the phylogenetic relatedness of the sequences amplified by each pair of primers was inferred using the Mega X package v11.0.13 [52]. A phylogenetic tree of each amplicon was inferred by using the Maximum Likelihood method, and the Hasegawa–Kishino–Yano [53], Jukes–Cantor [54], or Tamura 3-parameter [55] models were implemented accordingly. The bootstrap consensus tree was inferred from 1000 replicates.

**Table 2.** Geographical location of the whole genome WSSV sequences retrieved for this study.

GenBank Accession Number	Geographic Location
AF332093	China
AF369029	Thailand
AF440570	Taiwan
AP027283	Japan
AP027288	Japan
AP027290	Japan
JX515788	South Korea
KT995472	China
KU216744	Mexico
KX686117	China
MF768985	Australia
MG264599	Brazil
MG702567	India
MH090824	Ecuador
MN840357	China

#### 2.2.4. Physicochemical Parameters

The physicochemical properties of the primers (% GC, length,  $T_m$ ,  $\Delta G$ , self-complementarity, potential intra-molecular hairpin loop formation, and self-annealing of 3' and 5' ends) were analyzed with the OligoCalc online [56]. Primers and salt ( $\text{Na}^+$ ) concentrations were set according to the protocol for each pair of primers.

### 3. Results

#### 3.1. Primer Mapping

This study analyzed a variety of primers designed to detect WSSV to evaluate its performance *in silico*. As shown in Figure 1, these primers target the following regions of the WSSV genome: ORF WSV058 (encoding for the structural protein VP24), ORF WSV285 (according to sequence AF332093 from China), ORF WSSV419 (encoding for the protein VP664), and ORF WSSV480 (encoding for the structural protein VP28). Interestingly, even though it has been suggested that the putative function of the protein encoded by ORF285 might be similar to that of VP28 [57], this still needs to be confirmed.



**Figure 1.** Schematic representation of the circular genome of the WSSV isolate from Taiwan (GenBank acc. No. AF440570). Gray arrows indicate the position of the ORFs encoding for VP24, WSSV285, VP664 and VP28. Black lines represent the fragments amplified by the analyzed primers. 6: [18], 5: [22], 9: [23], 3: [43], 2: [42], 7: [45], 4: [44], 8: [46], 1: [41], and 5: [40].

### 3.2. Primer Specificity

The specificity of the primers analyzed in the current study was assessed by performing similarity searches of sequence databases for unintended targets using an in silico PCR amplification tool [47]. The stringency parameters of the analysis were tightened up so that at least one primer must have at least two total mismatches, including at least two mismatches at the 3' end, and would not be ignored unless there were nine or more mismatches. Those amplifications with a predicted amplicon size similar to the targeted amplicon were considered nonspecific. The highest number of hits obtained by the Primer-Blast search was 36,827 (for primers VP28-140Fw–VP28-140Rv, designed by Mendoza-Cano et al. [23]), and the lowest number of hits (7857) was identified for primers WSSV-RT1–WSSV-RT2 [45] (Table 3). Furthermore, primers VP28-140Fw and VP28-140Rv yielded the highest number of filtered hits (126), while primers FQ-P3–FQ-P4 [44] returned the lowest number of filtered hits (44). The primers WSS1011F–WSS1079R, RT-WSSV-F154–RT-WSSV-R154, P3–P4, WSSV-RT1–WSSV-RT2, and F–R, showed multiple mismatches when blasted against WSSV sequences (Supplemental Material). No unspecific amplifications were detected by using the primers analyzed.

**Table 3.** Primer specificity assessed by a similarity search. Total numbers of hits returned through a Primer-Blast search this study.

Primer	Number of Blast Hits Analyzed	Filtered Hits	Mismatches	Number of Nonspecific Amplifications
146F1-146R1	16,581	45	No	0
146F2-146R2	30,191	56	No	0
WSS1011F-WSS1079R	12,224	81	Yes	0
RT-WSSV-F154-RT-WSSV-R154	9819	61	Yes	0
WSSV341F-WSSV341R	13,699	47	No	0
P1-P2	21,128	47	No	0
P3-P4	20,724	52	Yes	0
FQ-P3-FQ-P4	9141	44	No	0
WSSV-RT1-WSSV-RT2	7857	45	Yes	0
F-W	16,758	109	Yes	0
VP28-140Fw-VP28-140Rv	36,827	126	No	0

### 3.3. Predicted Melt Curves of Amplicons

The observed melt profiles of the amplicons generated *in silico* were predicted using the uMelt web application (Figure 2). A melting profile with a single peak was only detected in six of the eleven virtual amplicons (Figure 2A,E,F,H–J). Multiple melt peaks from a single amplicon were detected using the primers WSSV341F–WSSV341R (two peaks at 83.5 and 85.25 °C) (Figure 2B), P1–P2 (three peaks at 83, 87, and 89 °C) (Figure 2C), P3–P4 (two peaks at 86 and 89 °C) (Figure 2D), and 146F2–146R2 (two peaks at 87 and 91 °C) (Figure 2G). Furthermore, differences in the melt temperatures of the peaks detected using the primers P1–P2 were detected when the amplicons generated were obtained from the sequences from Taiwan, Thailand, and China (GenBank acc. Nos. AF440570, AF369029, and AF332093, respectively). Thus, the virtual amplicons generated using the sequences from China and Thailand showed three peaks with melt temperatures of 82, 87, and 89 °C.

### 3.4. Phylogenetic Analysis of the Amplicons

A total of seven segments of the WSSV genome (corresponding to the 10 sets of primers analyzed in the current study) located in four distinctive ORFs were aligned and analyzed phylogenetically. The resulting phylogenetic trees (Figure 3) revealed that WSSV has undergone multiple mutations, deletions, and insertions, generating genotype variations. The greatest average genetic distance (62.33%) was found for the sequence amplified by primers P1–P2 of Kimura et al. [43], and the smallest genetic distance (80%) was found on the sequences amplified by primers VP28-140Fw–VP28140RV designed by Mendoza-Cano et al. [23], WSSV-RT1–WSSV-RT2 designed by Zhu and Quan [45], FQ-P3–FQ-P4, designed by Yuan et al. [44], Fw–Rv designed by Sivakumar et al. [46], and RTWSSVF154–RTWSSVR154 designed by Jang et al. [41]. Interestingly, the most significant variation in the clustered sequences was found in the WSSV sequences of Japan (2018–2022), Thailand (1996), Taiwan (1994), Korea (2011), and India (2013).

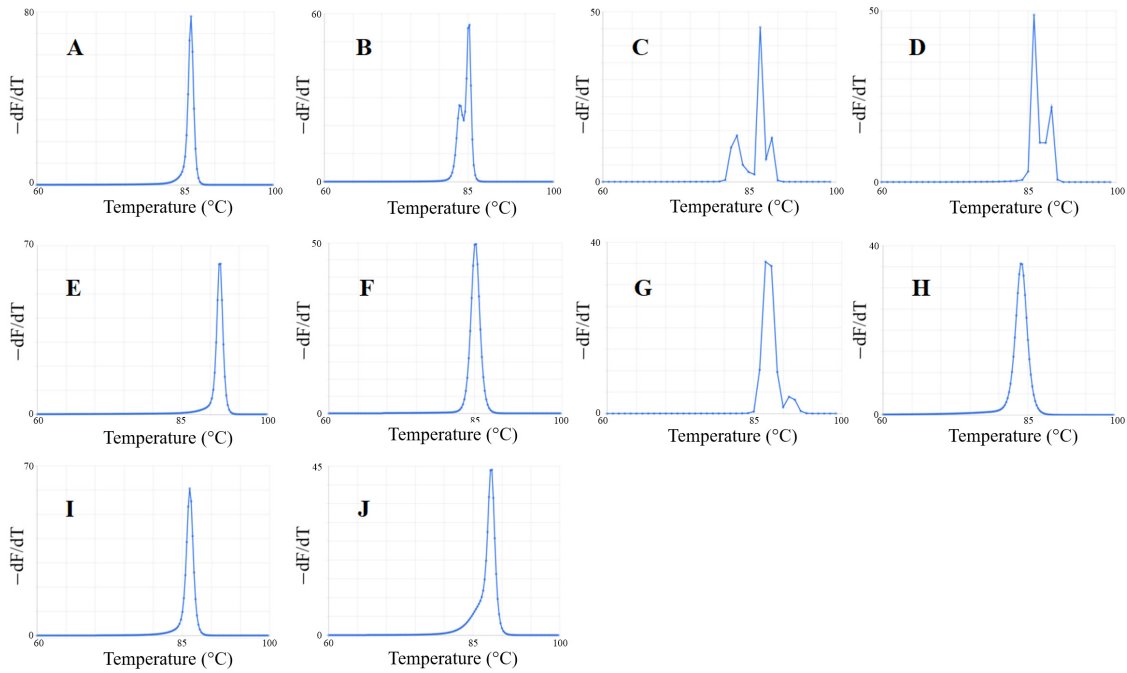


**Figure 2.** Predicted melt curves of the PCR products amplified with the primers analyzed in the current study. The plots were generated using uMelt under default parameters. (F): [18]; (G): [22]; (J): [23]; (D): [43]; (B): [42]; (H): [45]; (E): [44]; (I): [46]; (A): [41], and (C): [43].

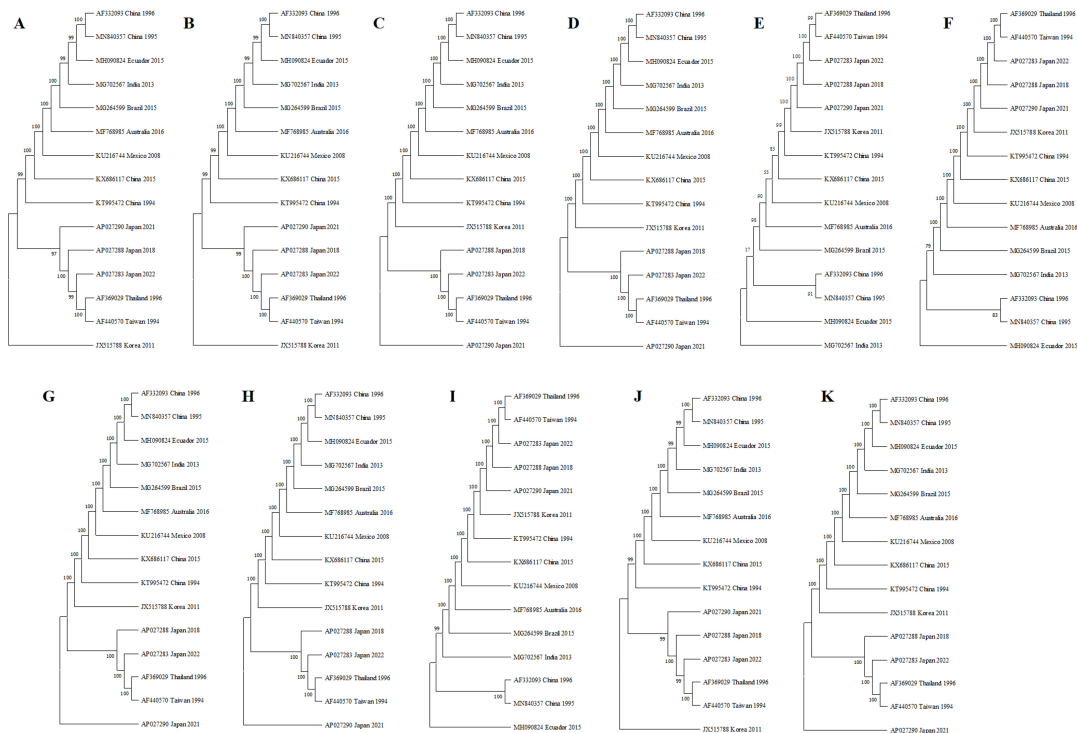


**Figure 3.** Phylogenetic trees of the sequences amplified by the different sets of primers analyzed in the current study. The percentage of replicate trees in which the associated taxa clustered together in the bootstrap test (1000 replicates) are shown next to the branches. (J): [18] (WSSV1011F–WSSV1079R); (A): [22] (146F1–146R1); (B): [22] (146F2–146R2); (H): [23] (VP28-140Fw–VP28-140Rv); (E): [43] (P1–P2); (F): [43] (P3–P4); (I): [42] (WSSV341F–WSSV341R); (K): [45] (WSSV-RT1–WSSVRT2); (C): [44] (FQ-P3–FQ-P4); (D): [46] (Fw–Rv); and (G): [41] (RT-WSSV-F154–RT-WSSV-R154).

### 3.5. Physicochemical Properties of Primers

As several properties of the primers contribute to defining their ability to specifically hybridize with the targeted sequence, some characteristics, such as their GC content, binding capacity ( $\Delta G$ ), and length, were also tested *in silico* to estimate their performance. As shown in Table 4, the lowest GC content (39%) was detected in the primer 146F1, and the highest GC content (61%) was detected in the primer WSSV-RT2. Furthermore, the shortest length of a primer was found in the oligonucleotide WSSV-RT2 (18 nt), while 146R1 was the most extended primer (25 nt). In addition, the primer 146R2 showed the highest  $T_m$  (62.57 °C), and the lowest  $T_m$  was estimated for primer VP28-140Rv (52.25 °C). The highest calculated binding affinity, in terms of its  $\Delta G$ , of the primers analyzed in the current study was observed in primer 146R2 (−32.3), whereas the lowest  $\Delta G$  was estimated for primer P3 (−23.8). This analysis also showed that two primers (146R2 and VP28-140Fw) contain internal regions that may lead to some degree of self-complementarity. Moreover, the 146R2 primer showed the potential to form hairpin loop structures. Finally, three primers (146R2, FQ-P3, and Fw) could potentially perform self-annealing of 3' and 5' ends.

**Table 4.** Primer specificity assessed by a similarity search. Total numbers of hits returned through a Primer-Blast search this study. SD: Self-dimer formation, HF: Hairpin formation, SA: Self-annealing.

Primer	GC (%)	Length (bp)	$T_m$ (°C)	$\Delta G$ (Kcal/mol)	SD	HF	SA
146F1	39	23	52.67	−26.0	-	-	-
146R1	40	25	56.74	−32.0	-	-	-
146F2	55	22	56.22	−29.1	-	-	-
146R2	59	22	62.57	−32.3	✓	✓	✓
WSS1011F	60	20	57.38	−27.2	-	-	-
WSS1079R	53	19	56.04	−25.5	-	-	-
RT-WSSV-F154	50	20	54.82	−26.2	-	-	-
RT-WSSV-R154	50	20	55.16	−26.3	-	-	-
WSSV341F	50	20	56.43	−25.4	-	-	-
WSSV341R	60	20	58.46	−27.2	-	-	-
P1	50	20	54.94	−25.2	-	-	-
P2	55	20	55.21	−25.8	-	-	-
P3	45	20	53.29	−23.8	-	-	-
P4	45	20	52.75	−24.6	-	-	-
FQ-P3 (up)	52	21	59.38	−27.9	-	-	✓
FQ-P4 (down)	55	20	57.63	−26.7	-	-	-
WSSV-RT1	45	20	53.72	−25.6	-	-	-
WSSV-RT2	61	18	54.0	−24.3	-	-	-
Forward	50	22	55.45	−27.7	-	-	✓
Reverse	50	20	54.83	−25.8	-	-	-
VP28-140Fw	45	22	53.39	−27.4	✓	-	-
VP28-140Rv	45	20	52.25	−24.7	-	-	-

## 4. Discussion

Due to its commercial significance, several crustacean species are exported across international borders. During the last decades, the remarkable growth of the shrimp farming industry has stimulated the international movement of shrimp species. This transboundary transportation of organisms enables the introduction of infective microorganisms with high

pathogenic potential into areas where they previously have not been found, affecting naïve host populations. Thus, WSSV was introduced into the Americas in 1995 through imported frozen shrimp from China to Texas, affecting local populations of crayfish (*Orconectes punctimanus* and *Procambarus sp.*), crabs (*Callinectes sapidus*), and shrimp (*Penaeus setiferus*, *P. aztecus*, and *P. vannamei*), between 1995 and 2004 [58]. Moreover, it has been demonstrated that the global dispersal of shrimp viral pathogens could occur through additional routes, including the international sale of infected nauplii, postlarvae and broodstock, ship ballast water, and shrimp packing-plant wastes [58].

Hence, in the Manual of Diagnostic Tests for Aquatic Animals, the World Organization for Animal Health has published standardized tests recommended for diagnosing specific diseases, which contribute, among other things, to preventing the spread of pathogens. Furthermore, this Manual lists diseases that should be mandatorily notifiable to the WOA, including WSSV. However, it has been reported that the PCR method described by Lo et al., [22] and recommended for detecting WSSV by WOA can lead to false-positive results in the red-claw crayfish *Cherax quadricarinatus* [34]. Thus, the WOA subsequently established in 2019 that all diagnostic assays should be first validated for the species in which they are intended to be used, and this validation should consider estimates of the analytical and diagnostic performance characteristics of the test.

We understand that there is no “ideal” diagnostic test for detecting WSSV, as its performance depends upon several conditions, such as the technical proficiency of the members of the laboratory or the species tested. However, evaluating the effectiveness of the existing diagnostic tests is an essential step toward setting high standards of quality and safety, which could help improve the production of this industry.

In total, 10 PCR protocols for the detection of WSSV were analyzed in silico in the current study. When the number of hits and filtered hits obtained by Blast were analyzed, it was clear that the specificity of the primers designed by Mendoza-Cano and Sánchez-Paz [23] was the highest. It is important to note that a query sequence is said to “hit” a target sequence if they match subsequences (termed high-scoring segment pair or HSP), which implies that a Blast search often contains many redundant HSPs [59]. Therefore, it seems reasonable to assume that a portion of the 36,827 hits detected with the primers VP28-140Fw–VP28-140Rv could be redundant sequences. However, once all the redundant genomic hits were removed, this set of primers still showed the highest number of filtered hits (126), indicating that, when compared to the other primers, the protocol described by Mendoza-Cano and Sánchez-Paz [23] recognizes numerous regions of similarity between WSSV sequences.

Interestingly, when the primers WSS1011F–WSS1079R [18], RT-WSSV-F154–RT-WSSV-R154 [41], P3–P4 [43], WSSV-RT1–WSSV-RT2 [45], and F–R [46] were blasted against WSSV sequences numerous mismatches were found. Several studies have demonstrated that increasing mismatches in a primer could reduce the amplification efficiency, quantification cycle ( $C_q$ ), and quantification accuracy of PCR [60–62].

The in silico melt profiles of the amplicons generated performing the different amplification protocols with the sets of primers analyzed in the current study showed that while only six of the virtual amplicons generated a single peak, the primers WSSV341F–WSSV341R [42], P1–P2 [43], P3–P4 [43], and 146F2–146R2 [22] could generate multiple melt peaks. It should be noted, however, that even though the presence of multiple peaks is not necessarily indicative of nonspecific amplification, it could contribute to predict, and avoid, amplification artifacts that may affect the accuracy of the diagnosis.

The PCR is a procedure that intrinsically could result in biases and errors attributable to factors such as annealing between primers, self-annealing of primers, and the formation of chimeric sequences [63]. Thus, several parameters of the primers, such as their melting temperature, GC content, self-annealing, and annealing between primers, should be carefully analyzed to obtain accurate results if they are intended to be used in diagnostics. In general terms, some characteristics of the primers studied are suitable to accurately detect WSSV. However, the in silico analysis of secondary structures within/between

primer pairs suggested that some primers, particularly 146R2, showed the potential for self-annealing and forming hairpin loop structures. This affects the PCR efficiency and accuracy in the detection of WSSV. Furthermore, under certain circumstances, it could lead to false-positive results.

Interestingly, the primers of these protocols target four ORFs (WSSV058, ORF285, WSSV419, and WSSV480). The primers described by Jang et al. [41], named RT-WSSV-F154 and RT-WSSV-R154, target a segment of ORF WSSV058, which encodes for VP24, one of the major envelope proteins of WSSV [64–66]. VP24 is a chitin-binding protein essential for WSSV infection [67], and it acts as a core protein that directly associates with five other structural proteins (VP26, VP28, VP38A, VP51A, and WSV010) to form a membrane-associated protein complex known as the “infectome” [68]. When genomic sequences from 15 different geographical regions covering the amplified product by this set of primers were aligned, it was observed that this fragment of the VP24 is highly conserved. A plausible explanation for this could be that due to its critical role in contributing to the binding and entry of the virus into its host cells, some regions of this protein should be highly conserved (or show a low evolutionary rate) since changes in its sequence may affect the viral fitness. However, the specificity of primers RT-WSSV-F154 and RT-WSSV-R154 was low. After reviewing the amplification conditions of this assay, it is clear that the proposed protocol is adequate and could hardly be improved. However, according to the findings in this study, their specificity is low, which could be experimentally tested using samples from different geographic regions and other hosts for WSSV.

The primers described by Durand and Lightner [18], Lo et al. [22], Nunan and Lightner [40], Yuan et al. [44], and Zhu and Quan [45], target different regions of the ORF wsv419, which encodes VP664, the major WSSV structural protein of the nucleocapsid and the largest viral structural protein known, which is distributed with a periodicity that matches the characteristic stacked ring subunits that appear as striations [69]. The alignment of the sequences that the primers described by Durand and Lightner [18] amplify is highly conserved, with no gaps or insertions detected. From our perspective, this set of primers should be included as a reference for WSSV detection by the WHOA. On the contrary, when the sequence amplified by the primers 146F1–146R1 described by Lo et al. [22] from 15 geographically different regions were aligned, several insertions, gaps, transition mutations (interchange between two-ring purines or between one-ring pyrimidines) and transversion mutations (interchange of purine for pyrimidine bases) were found. It is worth noting that most deletions and insertions were found on the sequence MG702567 of a WSSV isolated from India in 2013, while the transition and transversion mutations were distributed among sequences AP027283 (Japan), JX515788 (Korea) and MG702567 (India). These changes may affect the detection results (i.e., the size of the amplicon of the Indian isolate would be ~20 nt smaller). Not surprisingly, since the primers 146F2–146R2 [22] are used in a nested-PCR to allegedly increase sensitivity, targeting the same region of VP664 as primers 146F1–146R1, they undergo the same distinguishing features. Interestingly, Nunan and Lightner [40] optimized the protocol described by Lo et al. [22]. Thus, the annealing temperature of primers 146F2–146R2 was adjusted from 55 °C to 62 °C, and the cycling times were shortened from 40 to 30 cycles. This set of primers was tested against various WSSV isolates from different geographical locations (Honduras, USA, Brazil, Indonesia, Hawaii, Nicaragua, and China) to assess its accuracy in detecting WSSV. However, the sequences of some new isolates have been reported, demonstrating that this virus has evolved. Thus, the amplicons generated by this set of primers could show a different electrophoretic behavior than previously observed.

The primers FQ-P3 and FQ-P4, described by Yuan et al. [44], target a 129 bp fragment of the WSSV ORF encoding VP664. A single gap was detected in sequence MG702567 (from India).

According to Zhu and Quan [45], the primers WSSV-RT1 and WSSV-RT2 should yield a PCR product of 154 bp; however, when the target sequences of both primers were analyzed *in silico*, the real size of the amplicon is 57 bp, revealing a striking difference. Alignment of

the sequences from different geographic locations amplified in silico by this set of primers showed a single deletion near the 5'-end of the MG702567 sequence (India). It is well known that complementarity between primers and the template is a fundamental factor for PCR applications, as mismatches can lead to inefficient amplification of targeted regions of the DNA template [70]. Furthermore, it has been reported that primers containing a single base mismatch near the 3'-end of the primer can significantly underestimate (~3 logs) the estimated viral load of a sample [71]. It is worth noting that under certain circumstances, these difficulties can be suppressed by adjusting the temperature of the annealing steps. Thus, considering the increasing genetic diversity observed in WSSV isolates, the annealing temperature (52 °C) reported in the amplification protocol described by Zhu and Quan [45] could be slightly increased to improve its specificity.

The primers designed by Kimura et al. [43] and Tang and Lightner [42] amplify a fragment of the ORF WSV285. It has been suggested that the protein encoded by this gene could have a similar function to that of VP28 [57]. As demonstrated here, in comparison with other primers, those designed by Kimura et al. [43], P1–P2 and P3–P4, amplify a genomic segment of the ORF WSV285, that is the most polymorphic region among those analyzed here. More than 30 changes (deletions, transitions, and transversions) were found distributed in sequences AFF440570 (Taiwan), MG702567 (India), MF768985 (Australia), KX686117 (China), and MH090824 (Ecuador). Thus, when primers P1–P2 were used to amplify sequences MG702567 and KX686117, the sizes of the amplicons were 20 and 3 bases shorter than the others, respectively.

Finally, the primers designed by Mendoza-Cano and Sánchez-Paz [23] and Sivakumar et al. [46] target the major structural protein of WSSV, VP28. This viral protein is widely recognized as essential for a successful viral infection since it participates in cell recognition and attachment and cytoplasm entry during infection [11,23,72–75] and in virion assembly and morphogenesis [64,76,77]. The multiple alignment of the sequences targeted by the primers designed by Sivakumar et al. [46] showed a single transition mutation in sequence MF768985 (Australia) near the 3'-end of the Forward primer. On the contrary, no variations were observed in any of the geographically different sequences amplified by the primers described by Mendoza-Cano and Sánchez-Paz [23]. In agreement with this finding, it should be noted that this set of primers (VP28-140Fw and VP28-140Rw) were experimentally tested previously against isolates from different geographical origins (Brazil, China, Madagascar, Saudi Arabia, and Mexico), and in all cases, there was a specific detection of WSSV [23]. The sequence alignments, together with the topologies of phylogenetic relationships among the genomes of the WSSV isolates analyzed here, suggest fluctuating evolutionary rates (perhaps under distinctive selective pressures or recombination) at different genome sites of the WSSV. Viruses, like any other biological species, evolve, which implies that the design of primers should consider the analysis and selection of genomic regions with low mutability and their expression patterns. Thus, the primers described by Mendoza-Cano and Sánchez-Paz [23] were designed from a sequence encoding a segment of the VP28 protruding outside the viral envelope, which has been suggested to exert an essential role in the initial interaction with host receptors. Due to its probable essential role in mediating viral entry, amino acid changes in the structure of this segment of the envelope protein may alter the binding affinity for host receptors, compromising viral fitness. Thus, few changes may be expected to occur naturally in this protein, providing unique regions that will aid in the detection of this lethal virus.

The evolutionary relationships of the WSSV sequences amplified by the primers are shown in Figure 3. These relationships emphasize the growing diversity of this virus. A recent study found an increase from 33 to 39 families of crustaceans that could be infected by WSSV (in addition, 11 families of non-crustacean hosts could act as potential vectors of this virus) [10], which highlights that this viral pathogen continues to spread beyond farmed shrimp and the shrimp pond environment. Taken together, these variations suggest that the continuous spread of WSSV through different hosts and regions could have impacted

its evolutionary history, which implies that the detection protocols should be continuously reviewed and actualized to maintain proper surveillance.

## 5. Conclusions

As mentioned above, Claydon et al. [34] reported that the primers recommended by OIE yielded false-positive results in specimens of *C. quadricarinatus*. To the best of our knowledge, the only set of primers tested in different crustacean species is that reported by Mendoza-Cano and Sánchez-Paz [23]. Considering the growing number of hosts and vectors of WSSV (some of which could be introduced in shrimp farming facilities), the WOA should incorporate, in the Manual of Diagnostic Tests for Aquatic Animals, new protocols that have confirmed their suitability for the detection of this pathogen in other crustacean species that may serve as vectors of WSSV, which satisfies, at the end, one of the purposes of the Manual: the prevention of the spread of pathogens.

**Supplementary Materials:** The following supporting information can be downloaded at: <https://www.mdpi.com/article/10.3390/fishes9010005/s1>. Information of Primers.

**Author Contributions:** Conceptualization, F.M.-C.; methodology and software, F.M.-C. and T.E.-G.; writing—original draft preparation, A.S.-P.; writing—review and editing, A.S.-P. and T.E.-G.; supervision, A.S.-P. All authors have read and agreed to the published version of the manuscript.

**Funding:** This research received no external funding.

**Data Availability Statement:** Data sharing applicable upon request.

**Acknowledgments:** We greatly appreciate the valuable assistance provided by Ing. Juan Vega Peralta. We also thank the valuable support provided by Rosa María Valenzuela, Ing. Rodolfo Barraza, Alfredo Barreras Torres, Irma Soto and Claudia Cabrera from CIBNOR Hermosillo. We sincerely appreciate the contribution of Ana Paulina Salazar Cordova from Universidad de Sonora (Ciencias Genómicas).

**Conflicts of Interest:** The authors declare no conflicts of interest.

## References

- Dey, B.K.; Dugassa, G.H.; Hinzano, S.M.; Bossier, P. Causative agent, diagnosis, and management of white spot disease in shrimp: A review. *Rev. Aquacult.* **2020**, *12*, 822–865. [CrossRef]
- Zhang, X.; Hu, L.H.; Song, D.W.; Hu, Y.; Chen, J. Evaluation on prevention and treatment of cuminaldehyde in culture of shrimp against white spot syndrome virus. *Aquaculture* **2023**, *562*, 738760. [CrossRef]
- Stentiford, G.D.; Neil, D.M.; Peeler, E.J.; Shields, J.D.; Small, H.J.; Flegel, T.W.; Vlak, J.M.; Jones, B.; Morado, F.; Moss, S.; et al. Disease will limit future food supply from the global crustacean fishery and aquaculture sectors. *J. Invertebr. Pathol.* **2012**, *110*, 141–157. [CrossRef] [PubMed]
- Flegel, T.W. Historic emergence, impact, and current status of shrimp pathogens in Asia. *J. Invertebr. Pathol.* **2012**, *110*, 166–173. [CrossRef] [PubMed]
- Millard, R.S.; Ellis, R.P.; Bateman, K.S.; Bickley, L.K.; Tyler, C.R.; van Aerle, R.; Santos, E.M. How do abiotic environmental conditions influence shrimp susceptibility to disease? A critical analysis focused on White Spot Disease. *J. Invertebr. Pathol.* **2021**, *186*, 107369. [CrossRef] [PubMed]
- van Hulten, M.C.; Witteveldt, J.; Peters, S.; Kloosterboer, N.; Tarchini, R.; Fiers, M.; Sandbrink, H.; Lankhorst, R.K.; Vlak, J.M. The white spot syndrome virus DNA genome sequence. *Virology* **2001**, *286*, 7–22. [CrossRef]
- Yang, F.; He, J.; Lin, X.; Li, Q.; Pan, D.; Zhang, X.; Xu, X. Complete genome sequence of the shrimp white spot bacilliform virus. *J. Virol.* **2001**, *75*, 11811–11820. [CrossRef] [PubMed]
- Leu, J.H.; Yang, F.; Zhang, X.; Xu, X.; Kou, G.H.; Lo, C.F. Whispovirus. In *Lesser-Known Large dsDNA Viruses*; Van Etten, J.L., Ed.; Springer: Berlin/Heidelberg, Germany, 2009; pp. 197–227.
- Rozenberg, A.; Brand, P.; Rivera, N.; Leese, F.; Schubart, C.D. Characterization of fossilized relatives of the White Spot Syndrome Virus in genomes of decapod crustaceans. *BMC Evol. Biol.* **2015**, *15*, 142. [CrossRef]
- Desrina, Prayitno, S.B.; Verdegem, M.C.J.; Verreth, J.A.J.; Vlak, J.M. White spot syndrome virus host range and impact on transmission. *Rev. Aquacult.* **2022**, *14*, 1843–1860. [CrossRef]
- Sánchez-Paz, A. White spot syndrome virus: An overview on an emergent concern. *Vet. Res.* **2010**, *41*, 43. [CrossRef]
- Poulos, B.T.; Pantoja, C.R.; Bradley-Dunlop, D.; Aguilar, J.; Lightner, D.V. Development and application of monoclonal antibodies for the detection of white spot syndrome virus of penaeid shrimp. *Dis. Aquat. Organ.* **2001**, *47*, 13–23. [CrossRef]

13. Murugan, V.; Sankaran, K. Bacterial lipid modification of ICP11 and a new ELISA system applicable for WSSV infection detection. *Mar. Biotechnol.* **2018**, *20*, 375–384. [[CrossRef](#)]
14. Anil, T.M.; Shankar, K.M.; Mohan, C.V. Monoclonal antibodies developed for sensitive detection and comparison of white spot syndrome virus isolates in India. *Dis. Aquat. Organ.* **2001**, *51*, 67–75. [[CrossRef](#)]
15. Liu, W.; Wang, Y.T.; Tian, D.S.; Yin, Z.C.; Kwang, J. Detection of white spot syndrome virus (WSSV) of shrimp by means of monoclonal antibodies (MAbs) specific to an envelope protein (28 kDa). *Dis. Aquat. Organ.* **2002**, *49*, 11–18. [[CrossRef](#)]
16. You, Z.; Nadala, E.C.; Yang, J.; van Hulten, M.C.; Loh, P.C. Production of polyclonal antiserum specific to the 27.5 kDa envelope protein of white spot syndrome virus. *Dis. Aquat. Organ.* **2002**, *51*, 77–80. [[CrossRef](#)]
17. Sithigorngul, P.; Rukpratanporn, S.; Chaivisuthangkura, P.; Sridulyakul, P.; Longyant, S. Simultaneous and rapid detection of white spot syndrome virus and yellow head virus infection in shrimp with a dual immunochromatographic strip test. *J. Virol. Methods* **2011**, *173*, 85–91. [[CrossRef](#)]
18. Durand, S.V.; Lightner, D.V. Quantitative real time PCR for the measurement of white spot syndrome virus in shrimp. *J. Fish Dis.* **2002**, *25*, 381–389. [[CrossRef](#)]
19. Fouzi, M.; Shariff, M.; Omar, A.R.; Yusoff, F.M.; Tan, S.W. TaqMan real-time PCR assay for relative quantification of white spot syndrome virus infection in *Penaeus monodon* Fabricius exposed to ammonia. *J. Fish Dis.* **2010**, *33*, 931–938. [[CrossRef](#)]
20. Kim; Kim; Sohn; Sim; Park; Heo; Lee; Lee; Jun; Jang. Development of a polymerase chain reaction (PCR) procedure for the detection of baculovirus associated with white spot syndrome (WSBV) in penaeid shrimp. *J. Fish Dis.* **1998**, *21*, 11–17. [[CrossRef](#)]
21. Leal, C.A.G.; Carvalho, A.F.; Leite, R.C.; Figueiredo, H.C.P. Development of duplex real-time PCR for the detection of WSSV and PstDV1 in cultivated shrimp. *BMC Vet. Res.* **2014**, *10*, 150. [[CrossRef](#)]
22. Lo, C.F.; Ho, C.H.; Peng, S.E.; Chen, C.H.; Hsu, H.C.; Chiu, Y.L.; Chang, C.F.; Liu, K.F.; Su, M.S.; Wang, C.H.; et al. White spot syndrome baculovirus (WSBV) detected in cultured and captured shrimp, crabs, and other arthropods. *Dis. Aquat. Organ.* **1996**, *27*, 215–225. [[CrossRef](#)]
23. Mendoza-Cano, F.; Sánchez-Paz, A. Development and validation of a quantitative real-time polymerase chain assay for universal detection of the White Spot Syndrome Virus in marine crustaceans. *Virol. J.* **2013**, *10*, 186. [[CrossRef](#)] [[PubMed](#)]
24. Natividad, K.D.T.; Nomura, N.; Matsumura, M. Detection of White spot syndrome virus DNA in pond soil using a 2-step nested PCR. *J. Virol. Methods* **2008**, *149*, 28–34. [[CrossRef](#)] [[PubMed](#)]
25. Pan, X.; Zhang, Y.; Sha, X.; Wang, J.; Li, J.; Dong, P.; Liang, X. Highly sensitive detection of low-abundance White Spot Syndrome Virus by a pre-amplification PCR method. *J. Microbiol. Biotechnol.* **2017**, *27*, 471–479. [[CrossRef](#)] [[PubMed](#)]
26. Caipang, C.M.A.; Sibonga, M.F.J.; Geduspan, J.S.; Amar, M.J.A. An optimized loop-mediated isothermal amplification (LAMP) assay for the detection of white spot syndrome virus (WSSV) among cultured shrimps in the Philippines. *J. Anim. Plant Sci.* **2012**, *22*, 927–932.
27. Chou, P.H.; Lin, Y.C.; Teng, P.H.; Chen, C.L.; Lee, P.Y. Real-time target-specific detection of loop-mediated isothermal amplification for white spot syndrome virus using fluorescence energy transfer-based probes. *J. Virol. Methods* **2011**, *173*, 67–74. [[CrossRef](#)] [[PubMed](#)]
28. He, L.; Xu, H. Development of a multiplex loop-mediated isothermal amplification (mLAMP) method for the simultaneous detection of white spot syndrome virus and infectious hypodermal and hematopoietic necrosis virus in penaeid shrimp. *Aquaculture* **2011**, *311*, 94–99. [[CrossRef](#)]
29. Jaroenram, W.; Kiatpathomchai, W.; Flegel, T.W. Rapid and sensitive detection of white spot syndrome virus by loop-mediated isothermal amplification combined with a lateral flow dipstick. *Mol. Cel. Probes* **2009**, *23*, 65–70. [[CrossRef](#)]
30. Kono, T.; Savan, R.; Sakai, M.; Itami, T. Detection of white spot syndrome virus in shrimp by loop-mediated isothermal amplification. *J. Virol. Methods* **2004**, *115*, 59–65. [[CrossRef](#)]
31. Bai, Y.; He, L.; Sun, M.; Zhou, X.; Xu, Z. Dark-field visual counting of white spot syndrome virus using gold nanoparticle probe. *Aquaculture* **2023**, *562*, 738797. [[CrossRef](#)]
32. Etedali, P.; Behbahani, M.; Mohabatkar, H.; Dini, G. Field-usable aptamer-gold nanoparticles-based colorimetric sensor for rapid detection of white spot syndrome virus in shrimp. *Aquaculture* **2022**, *548*, 737628. [[CrossRef](#)]
33. WOA. Infection with White Spot Syndrome Virus. In *Manual of Diagnostic Tests for Aquatic Animals*; World Organisation for Animal Health: Paris, France, 2023; Chapter 2.2.8, pp. 1–17. Available online: [https://www.woah.org/fileadmin/Home/eng/Health\\_standards/aahm/current/2.2.08\\_WSSV.pdf](https://www.woah.org/fileadmin/Home/eng/Health_standards/aahm/current/2.2.08_WSSV.pdf) (accessed on 15 May 2023).
34. Claydon, K.; Cullen, B.; Owens, L. OIE white spot syndrome virus PCR gives false-positive results in *Cherax quadricarinatus*. *Dis. Aquat. Organ.* **2004**, *62*, 265–268. [[CrossRef](#)] [[PubMed](#)]
35. De Filippis, I.; de Azevedo, A.C.; de Oliveira Lima, I.; Ramos, N.F.L.; de Andrade, C.F.; de Almeida, A.E. Accurate, fast and cost-effective simultaneous detection of bacterial meningitis by qualitative PCR with high-resolution melting. *BioTechniques* **2023**, *74*, 101–106. [[CrossRef](#)] [[PubMed](#)]
36. Bustin, S.; Huggett, J. qPCR primer design revisited. *Biomol. Detect. Quantif.* **2017**, *14*, 19–28. [[CrossRef](#)] [[PubMed](#)]
37. Kalendar, R.; Khassenov, B.; Ramankulov, Y.; Samuilova, O.; Ivanov, K.I. FastPCR: An in silico tool for fast primer and probe design and advanced sequence analysis. *Genomics* **2017**, *109*, 312–319. [[CrossRef](#)] [[PubMed](#)]
38. Wang, C.H.; Lo, C.F.; Leu, J.H.; Chou, C.M.; Yeh, P.Y.; Chou, H.Y.; Tung, M.C.; Chang, C.F.; Su, M.S.; Kou, G.H. Purification and genomic analysis of baculovirus associated with white spot syndrome (WSBV) of *Penaeus monodon*. *Dis. Aquat. Organ.* **1995**, *23*, 239–242. [[CrossRef](#)]

39. Davis, M.W.; Jorgensen, E.M. ApE, A plasmid editor: A freely available DNA manipulation and visualization program. *Front. Bioinformatics* **2022**, *2*, 818619. [[CrossRef](#)]
40. Nunan, L.M.; Lightner, D.V. Optimized PCR assay for detection of white spot syndrome virus (WSSV). *J. Virol. Methods* **2011**, *171*, 318–321. [[CrossRef](#)]
41. Jang, I.K.; Meng, X.H.; Seo, H.C.; Cho, Y.R.; Kim, B.R.; Ayyaru, G.; Kim, J.S. A TaqMan real-time PCR assay for quantifying white spot syndrome virus (WSSV) infections in wild broodstock and hatchery-reared postlarvae of fleshy shrimp, *Fenneropenaeus chinensis*. *Aquaculture* **2009**, *287*, 40–45. [[CrossRef](#)]
42. Tang, K.F.J.; Lightner, D.V. Quantification of white spot syndrome virus DNA through a competitive polymerase chain reaction. *Aquaculture* **2000**, *189*, 11–21. [[CrossRef](#)]
43. Kimura, T.; Yamano, K.; Nakano, H.; Momoyama, K.; Hiraoka, M.; Inouye, K. Detection of Penaeid Rod-shaped DNA Virus (PRDV) by PCR. *Fish Pathol.* **1996**, *31*, 93–98. [[CrossRef](#)]
44. Yuan, L.; Zhang, X.; Chang, M.; Jia, C.; Hemmingsen, S.M.; Dai, H. A new fluorescent quantitative PCR-based in vitro neutralization assay for white spot syndrome virus. *J. Virol. Methods* **2007**, *146*, 96–103. [[CrossRef](#)] [[PubMed](#)]
45. Zhu, F.; Quan, H. A new method for quantifying white spot syndrome virus: Experimental challenge dose using TaqMan real-time PCR assay. *J. Virol. Methods* **2012**, *184*, 121–124. [[CrossRef](#)]
46. Sivakumar, S.; Vimal, S.; Abdul Majeed, S.; Santhosh Kumar, S.; Taju, G.; Madan, N.; Rajkumar, T.; Thamizhvanan, S.; Shamsudheen, K.V.; Scaria, V.; et al. A new strain of white spot syndrome virus affecting *Litopenaeus vannamei* in Indian shrimp farms. *J. Fish Dis.* **2018**, *41*, 1129–1146. [[CrossRef](#)] [[PubMed](#)]
47. Ye, J.; Coulouris, G.; Zaretskaya, I.; Cutcutache, I.; Rozen, S.; Madden, T.L. Primer-BLAST: A tool to design target-specific primers for polymerase chain reaction. *BMC Bioinform.* **2012**, *13*, 134. [[CrossRef](#)] [[PubMed](#)]
48. Dwight, Z.; Palais, R.; Wittwer, C.T. uMELT: Prediction of high-resolution melting curves and dynamic melting profiles of PCR products in a rich web application. *Bioinformatics* **2011**, *27*, 1019–1020. [[CrossRef](#)]
49. SantaLucia, J. A unified view of polymer, dumbbell, and oligonucleotide DNA nearest-neighbor thermodynamics. *Proc. Natl. Acad. Sci. USA* **1998**, *95*, 1460–1465. [[CrossRef](#)]
50. Katoh, K.; Standley, D.M. MAFFT multiple sequence alignment software version 7: Improvements in performance and usability. *Mol. Biol. Evol.* **2013**, *30*, 772–780. [[CrossRef](#)]
51. Sela, I.; Ashkenazy, H.; Katoh, K.; Pupko, T. GUIDANCE2: Accurate detection of unreliable alignment regions accounting for the uncertainty of multiple parameters. *Nucleic Acids Res.* **2015**, *43*, W7–W14. [[CrossRef](#)]
52. Kumar, S.; Stecher, G.; Li, M.; Knyaz, C.; Tamura, K. MEGA X: Molecular Evolutionary Genetics Analysis across computing platforms. *Mol. Biol. Evol.* **2018**, *35*, 1547–1549. [[CrossRef](#)]
53. Hasegawa, M.; Kishino, H.; Yano, T. Dating of the human-ape splitting by a molecular clock of mitochondrial DNA. *J. Mol. Evol.* **1985**, *22*, 160–174. [[CrossRef](#)] [[PubMed](#)]
54. Jukes, T.H.; Cantor, C.R. Evolution of protein molecules. In *Mammalian Protein Metabolism*; Munro, H.N., Ed.; Academic Press: New York, NY, USA, 1969; pp. 21–132.
55. Tamura, K. Estimation of the number of nucleotide substitutions when there are strong transition-transversion and G+C-content biases. *Mol. Biol. Evol.* **1992**, *9*, 678–687. [[CrossRef](#)] [[PubMed](#)]
56. Kibbe, W.A. OligoCalc: An online oligonucleotide properties calculator. *Nucleic Acids Res.* **2007**, *35*, W43–W46. [[CrossRef](#)] [[PubMed](#)]
57. Dang, L.T.; Koyama, T.; Shitara, A.; Kondo, H.; Aoki, T.; Hirono, I. Involvement of WSSV–shrimp homologs in WSSV infectivity in kuruma shrimp: *Marsupenaeus japonicus*. *Antivir. Res.* **2010**, *88*, 217–226. [[CrossRef](#)] [[PubMed](#)]
58. Hasson, K.W.; Fan, Y.; Reisinger, T.; Venuti, J.; Varner, P.W. White-spot syndrome virus (WSSV) introduction into the Gulf of Mexico and Texas freshwater systems through imported, frozen bait-shrimp. *Dis. Aquat. Organ.* **2006**, *71*, 91–100. [[CrossRef](#)] [[PubMed](#)]
59. Zhang, H. Alignment of BLAST high-scoring segment pairs based on the longest increasing subsequence algorithm. *Bioinformatics* **2003**, *19*, 1391–1396. [[CrossRef](#)]
60. Boyle, B.; Dallaire, N.; MacKay, J. Evaluation of the impact of single nucleotide polymorphisms and primer mismatches on quantitative PCR. *BMC Biotechnol.* **2009**, *9*, 75. [[CrossRef](#)]
61. De Long, S.K.; Kinney, K.A.; Kirisits, M.J. qPCR assays to quantify genes and gene expression associated with microbial perchlorate reduction. *J. Microbiol. Methods* **2010**, *83*, 270–274. [[CrossRef](#)]
62. Ledeker, B.M.; De Long, S.K. The effect of multiple primer-template mismatches on quantitative PCR accuracy and development of a multi-primer set assay for accurate quantification of pcrA gene sequence variants. *J. Microbiol. Methods* **2013**, *94*, 224–231. [[CrossRef](#)]
63. Hongoh, Y.; Yuzawa, H.; Ohkuma, M.; Kudo, T. Evaluation of primers and PCR conditions for the analysis of 16S rRNA genes from a natural environment. *FEMS Microbiol. Lett.* **2003**, *221*, 299–304. [[CrossRef](#)]
64. Tsai, J.M.; Wang, H.C.; Leu, J.H.; Wang, A.H.; Zhuang, Y.; Walker, P.J.; Kou, G.H.; Lo, C.F. Identification of the nucleocapsid, tegument, and envelope proteins of the shrimp white spot syndrome virus virion. *J. Virol.* **2006**, *80*, 3021–3029. [[CrossRef](#)] [[PubMed](#)]
65. Xie, X.; Xu, L.; Yang, F. Proteomic analysis of the major envelope and nucleocapsid proteins of white spot syndrome virus. *J. Virol.* **2006**, *80*, 10615–10623. [[CrossRef](#)] [[PubMed](#)]

66. Zhou, Q.; Xu, L.; Li, H.; Qi, Y.P.; Yang, F. Four major envelope proteins of white spot syndrome virus bind to form a complex. *J. Virol.* **2009**, *83*, 4709–4712. [[CrossRef](#)] [[PubMed](#)]
67. Li, Z.; Li, F.; Han, Y.; Xu, L.; Yang, F. VP24 is a chitin-binding protein involved in White Spot Syndrome Virus infection. *J. Virol.* **2015**, *90*, 842–850. [[CrossRef](#)] [[PubMed](#)]
68. Chang, Y.S.; Liu, W.J.; Lee, C.C.; Chou, T.L.; Lee, Y.T.; Wu, T.S.; Huang, J.Y.; Huang, W.T.; Lee, T.L.; Kou, G.H.; et al. A 3D model of the membrane protein complex formed by the White Spot Syndrome Virus structural proteins. *PLoS ONE* **2010**, *5*, e10718. [[CrossRef](#)] [[PubMed](#)]
69. Huang, H.J.; Tang, S.L.; Chang, Y.C.; Wang, H.C.; Ng, T.H.; Garmann, R.F.; Chen, Y.W.; Huang, J.Y.; Kumar, R.; Chang, S.H.; et al. Multiple nucleocapsid structural forms of shrimp White Spot Syndrome Virus suggests a novel viral morphogenetic pathway. *Int. J. Mol. Sci.* **2023**, *24*, 7525. [[CrossRef](#)] [[PubMed](#)]
70. Green, S.J.; Venkatramanan, R.; Naqib, A. Deconstructing the polymerase chain reaction: Understanding and correcting bias associated with primer degeneracies and primer-template mismatches. *PLoS ONE* **2015**, *10*, e0128122. [[CrossRef](#)] [[PubMed](#)]
71. Whiley, D.M.; Sloots, T.P. Sequence variation in primer targets affects the accuracy of viral quantitative PCR. *J. Clin. Virol.* **2005**, *34*, 104–107. [[CrossRef](#)]
72. Robalino, J.; Payne, C.; Parnell, P.; Shepard, E.; Grimes, A.C.; Metz, A.; Prior, S.; Witteveldt, J.; Vlak, J.M.; Gross, P.S.; et al. Inactivation of White Spot Syndrome Virus (WSSV) by normal rabbit serum: Implications for the role of the envelope protein VP28 in WSSV infection of shrimp. *Virus Res.* **2006**, *118*, 55–61. [[CrossRef](#)]
73. Sritunyalucksana, K.; Wannapapho, W.; Lo, C.F.; Flegel, T.W. PmRab7 is a VP28-binding protein involved in white spot syndrome virus infection in shrimp. *J. Virol.* **2006**, *80*, 10734–10742. [[CrossRef](#)]
74. van Hulten, M.C.; Witteveldt, J.; Snippe, M.; Vlak, J.M. White spot syndrome virus envelope protein VP28 is involved in the systemic infection of shrimp. *Virology* **2001**, *285*, 228–233. [[CrossRef](#)] [[PubMed](#)]
75. Yi, G.; Wang, Z.; Qi, Y.; Yao, L.; Qian, J.; Hu, L. Vp28 of shrimp white spot syndrome virus is involved in the attachment and penetration into shrimp cells. *J. Biochem. Mol. Biol.* **2004**, *37*, 726–734. [[CrossRef](#)] [[PubMed](#)]
76. Durand, S.; Lightner, D.V.; Redman, R.M.; Bonami, J.R. Ultrastructure and morphogenesis of White Spot Syndrome Baculovirus (WSSV). *Dis. Aquat. Organ.* **1997**, *29*, 205–211. [[CrossRef](#)]
77. Liu, Q.H.; Ma, C.Y.; Chen, W.B.; Zhang, X.L.; Liang, Y.; Dong, S.L.; Huang, J. White spot syndrome virus VP37 interacts with VP28 and VP26. *Dis. Aquat. Organ.* **2009**, *85*, 23–30. [[CrossRef](#)]

**Disclaimer/Publisher’s Note:** The statements, opinions and data contained in all publications are solely those of the individual author(s) and contributor(s) and not of MDPI and/or the editor(s). MDPI and/or the editor(s) disclaim responsibility for any injury to people or property resulting from any ideas, methods, instructions or products referred to in the content.